Unexpected Fracture Behavior of Ultrasoft Associative Hydrogels Due to Strain-Induced Crystallization

Yuanyuan Wei, Jianzhu Ju, Costantino Creton, Tetsuharu Narita

https://doi.org/10.1021/acsmacrolett.3c00343
ACS Macro Lett. **2023**, 12, 1106−1111

Unexpected fracture behavior of ultra-soft associative hydrogels due to strain-induced crystallization

Yuanyuan Wei, Jianzhu Ju, Costantino Creton*, Tetsuharu Narita*

Laboratoire Sciences et Ingénierie de la Matière Molle, CNRS UMR 7615, ESPCI Paris, Sorbonne Université, PSL Université, 10 rue Vauquelin, 75005 Paris, France.

*Corresponding authors: Costantino.Creton@espci.fr, Tetsuharu.Narita@espci.fr.

KEYWORDS: Ultra-soft hydrogels, fracture, crystallization, local reinforcement

ABSTRACT: Strain-induced crystallization (SIC) is a well-known toughening strategy in elastomers but is rarely observed in hydrogels due to their high-water content and limited deformability. Here we report a phenomenon of SIC in highly swollen and associative hydrogels by introducing an extremely large deformation by indentation with a needle. Using in-situ birefringence imaging, we discovered that SIC occurs close to the needle tip upon large strain, displacing the nucleation of a crack from the needle tip to a position further away from the tip. The morphology of the fracture as well as the force to induce the gel fracture with the needle can be controlled by playing with temperature and crosslinking and hence triggering or not the SIC. Our discovery points to a future direction in creating SIC in highly swollen hydrogels, with potential implications for many biological material designs, and surgical injury prediction or prevention in associative tissues.

Hydrogels, networks of cross-linked polymer chains swollen in water, are of considerable research interest for biomedical applications.[1] Conventional chemically crosslinked hydrogels exhibit brittleness and to improve fracture resistance, various hydrogels synthesized with several reinforcement strategies have been developed, including double network hydrogels having sacrificial bonds,[2] slide-ring hydrogels whose crosslinking points are mobile,[3] and nanocomposite hydrogels with reversible chain absorption onto inorganic fillers.[4] These reinforcement strategies are also efficient in unswollen elastomers.[5]

One of the reinforcement mechanisms which is well-known for elastomers but rarely applied to swollen hydrogels is strain-induced crystallization (SIC). SIC is frequently observed in elastomers, such as natural rubber (NR), some polyester based thermoplastic polyurethanes, polypropylene during processing, and polyesters.[6-9] NR crystallizes thermally at low temperatures, such as -25 °Çin an un-deformed state, while crystallization by applying strain is possible at high temperatures and is reversible when the strain is released. [10, 11] The self-organization of SIC ahead of the crack tip during stretching endows NR with a very high fracture toughness due to a peculiar fracture behavior, such as stick-slip crack propagation or knotty tearing,[12, 13] where a secondary crack tends to propagate in the stretching direction (side-way) deviating from the standard precut direction, which is considered as a principal reinforcement mechanism.

One of the reasons for the limited number of reports on SIC in swollen hydrogels is the dilution of the polymers in the swollen hydrogels decreasing the close contact or association of the polymer chains. It is however possible to introduce crystalline domains in hydrogels either by the dry-anneal method,[14] or very recently, by stretching,[3] at the expense of relatively high polymer concentrations. It should be noted that flow-induced crystallization (FIC) can occur for solutions as well as for melts, of various crystalline polymers.[15] The mechanism of FIC has been clarified as the molecular chain orientation by shear. In the same manner as in SIC, flow induces the orientation of stretched chains resulting in a decrease in entropy and an easier crystallization. It can be deduced that very large nonlinear deformation is necessary, while in hydrogels it is experimentally inaccessible by conventional mechanical measurement, since the defects naturally present in hydrogels tend to create localized stress concentrations on certain chemical bonds at the molecular level in which polymer chains break before their maximum extension limit.[5, 16, 17]

In this work, we report the strain-induced crystallization in highly swollen poly (vinyl alcohol) (PVA) hydrogels upon large deformation induced by the indentation of a needle. We intend to clarify the role of applied strain and temperature on the occurrence of SIC, and how this phenomenon affects fracture behavior of hydrogels.

A PVA hydrogel (hydrolysis degree DH = 99 %, termed as PVA99) is synthesized as described in the Materials section, exhibiting a purely elastic character (G' is independent of

frequency) (Figure S1). Puncture tests were performed with a custom set-up schematically shown in Figure 1a. The indentation force as well as birefringence images were recorded as a function of indenter displacements d. From the force curve, a drop of the force is attributed to the fracture of the sample, at which the value of the force F_c and displacement d_c are taken as critical values (Figure 1b). Figure 1c presents a series of birefringence images taken at increasing needle insertion displacements d for the PVA99 hydrogel. We confirmed that before indentation no birefringence is visible since the as-prepared hydrogel is in an amorphous state (no image shown). With increasing indentation depth, the birefringence intensity along the indenter is enhanced, indicating the increasing concentration of oriented polymer chains (Figure 1c (i)). When the indenter displacement reaches the critical fracture value (d_c = 14 mm) (Figure 1c (ii)), a zone with lower intensity suddenly appears several millimeters above the indenter tip as indicated by the red arrow. Below and above this low-intensity zone, two bright zones are visible: one at the needle tip is sharp, and the other above the needle tip is broad. With further increase in the displacement (Figure 1c (iii) at d = 15 mm), the former seems to follow the displacement of the needle tip, the latter seems to exhibit relaxation, and it continues to move upwards with a velocity in the order of 1 mm/s. Surprisingly, a V-shaped birefringence pattern remains in the sample when the needle is removed after puncture (Figure 1c (iv)).

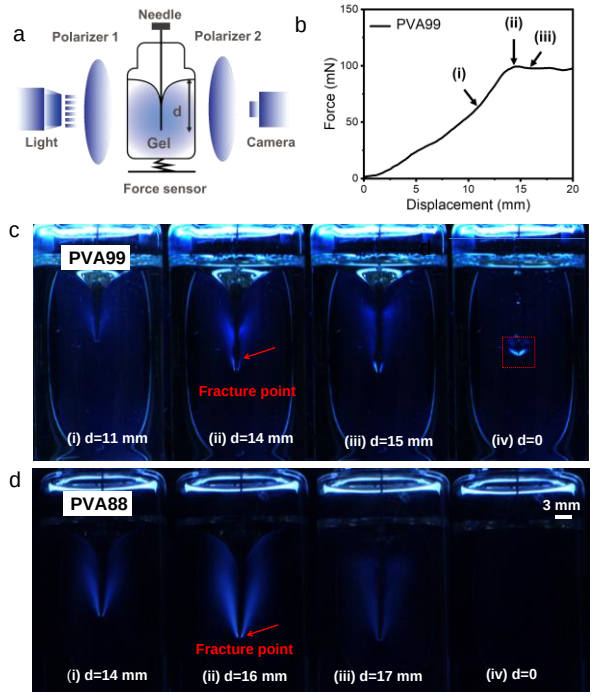

Figure 1. (a) Schematic of the custom puncture apparatus with birefringence imaging. (b) Puncture force as a function of displacement d for PVA99. Birefringence imaging under various indentation d for (c) PVA99 (G' = 400 Pa) and (d) PVA88 (G' = 800 Pa). d_c: fracture initiation; d = 0: pull-out of needle from sample.

The above-needle tip fracture behavior as well as the remaining V-shaped birefringence pattern is uniquely observed for PVA99 hydrogels when compared to PVA with a lower hydrolysis degree (DH = 88%, termed as PVA88). The birefringence intensity of PVA88 hydrogels disappears quickly at d_c, without exhibiting the above needle tip fracture nor permanent pattern when pulling out of needle after puncture (Figure 1d). We confirmed that several different hydrogels and elastomers, including polyacrylamide, and poly(dimethylsiloxane) (PDMS) (Figure S2) showed a similar puncture behavior as PVA88, consistent with what is typically found and reported in the literature, i.e. that the initiation of failure occurs in the compressed region below the tip.[18, 19] We also confirmed that there is no permanent birefringence pattern left for the PVA99 hydrogel fractured by a conventional uniaxial tension test (Figure S3) with a maximum stretch ratio $\lambda_c < 2$. On the contrary, in the puncture geometry, a very large strain is introduced to PVA99 at the fracture point, where $\lambda = d_c/R$ could reach ~ 60 (d_c = 14 mm and indenter radius R = 0.23 mm), demonstrating that the large strain may be responsible for the unique permanent birefringence pattern observed in PVA99 hydrogels.

To investigate the local strain state upon the occurrence of this V-shaped birefringence pattern, we performed cyclic puncture tests for the PVA99 hydrogel. The maximal displacement d_m of the cycle was increased stepwise and at each maximal displacement, two cycles were applied to evaluate the possible effect of irreversible damage. The value of d_m is below d_c thus no macroscopic fracture occurs. The time profile of the displacement and the birefringence images of the V-shaped pattern at varied values of d_m are shown in Figure 2a. A V-shaped pattern appears from d_m = 10 mm, and its intensity increases with d_m. It should be noted that reflected light from the gel surface was also detected and that the surface is not flat at d_m = 10 mm and higher, while it is flat at d_m = 5 mm. This result indicates that the gel surface deformed by indentation cannot fully relax upon withdrawal of the indenter when the V-shaped birefringence pattern (thus polymer chain orientation) exists and that the gel is *irreversibly* deformed. In fact, the V-shaped pattern is stable at room temperature over several months.

In order to evaluate the effect of the irreversible deformation on the mechanical behavior, the force curves were characterized and shown in Figure 2b. In Figure S4 curves for each value of d_m are shown. At d_m = 5 mm, the loading and unloading curves for the two cycles superpose well without hysteresis, indicating an elastic behavior without dissipation or damage. However, above d_m =10 mm, the unloading curves of the first cycle do not superpose on the corresponding loading curves thus hysteresis is observed (Figure 2b). With the increase in d_m, the hysteresis increases. This hysteresis behavior coincides with the appearance of a V-shaped pattern, and the level of birefringence intensity increases with the hysteresis, showing a power-law dependence with an exponent of about 0.5 (Figure 2c). Interestingly, no hysteresis behavior is observed, regardless of the applied maximum strain, for PVA88 hydrogel (Figure 2d), as expected for elastic hydrogels.

From the comparison of the two PVA samples, we assume that the V-shaped pattern could be attributed to strain-induced crystallization occurring upon the deep indentation process. PVA99 is (almost) fully hydrolyzed from poly(vinyl acetate). Hence it can be considered as an associative polymer due to inter- or inter-chain hydrogen bonding as schematically shown in Figure 2e. Such a polymer can crystallize in the dry state, or in an aqueous solution upon freezing,[20, 21] due to hydrophilic hydroxyl groups forming both inter- and intra- molecular hydrogen bonds.[22, 23] PVA88 is only partially hydrolyzed from poly (vinyl acetate) and contains 12 mol% acetate groups, along with 88 mol% percent hydroxyl groups. The hydrogen bond association in PVA88 is largely prevented by the bulky and hydrophobic acetate groups.[24] In fact, the formation of a physical gel by the freezing-thawing method cannot occur with PVA88.[25] Note that it was reported that in vulcanized natural rubber the mechanical hysteresis resulted only from a delay between chain crystallization upon loading and crystal melting upon unloading. [11, 26] The tough slide-ring hydrogels exhibiting SIC do not practically show mechanical hysteresis or residual strain, due to the rapid formation and destruction of the PEG crystallites.[3] For the PVA99 system, we suspect that the strong hydrogen bonding associations in PVA99 hydrogel can fix the strain serving as noncovalent crosslinks, preventing quick elastic recovery of the chain deformation, which results in the hysteresis behavior as well as the formation of the stable V-shaped anisotropic structure. Up to the rupture, the hydrogen bonding is enhanced as the deformation due to indentation increases and the stress is further concentrated at the needle tip, i.e., the strain-induced anisotropic structure, depicted as a V-shape birefringence pattern, is visualized.

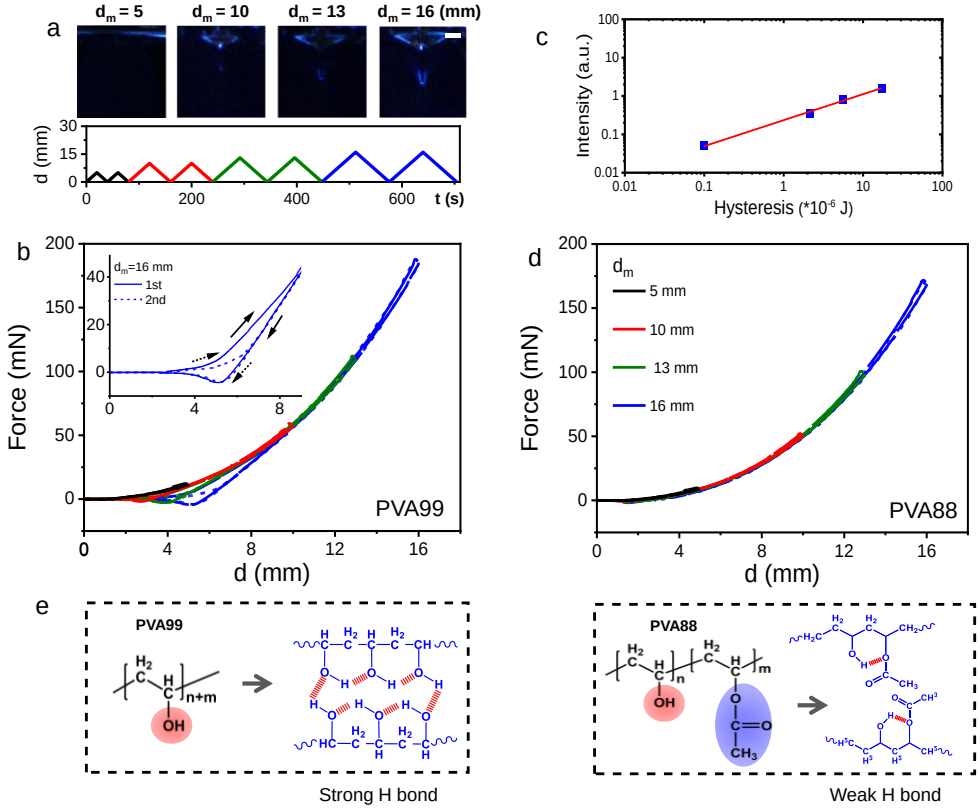

Figure 2. (a) Birefringence images after needle pull-out at various d_m for PVA99 (G' = 900 Pa) and the cyclic loading/unloading time profile. The scale bar is 3 mm. (b) Cyclic force curves for PVA99. (c) Birefringence intensity against hysteresis area. (d) Cyclic force curves for PVA88. (e) Schematic demonstrating strong hydrogen bonding in PVA99 and weak hydrogen bonding in PVA88.

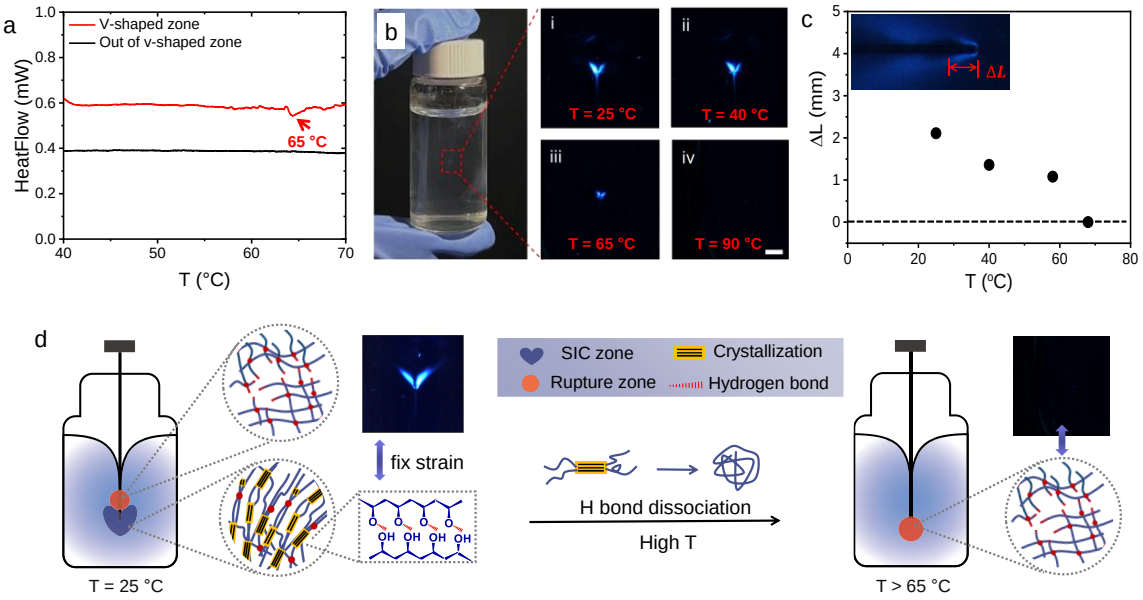

Figure 3. (a) Calorimetric thermograms during the heating process for the hydrogel in and out of the V-shaped zone. (b) V-shaped pattern at different temperatures. The scale bar is 3 mm. (c) Distance between the needle tip and the crack initiation position, ΔL, as a function of temperature. (d) Schematic illustration of strain-induced crystallization around the needle tip and resulting above-tip crack behavior at T = 25 °C and T > 65 °C.

To investigate the origin of this anisotropic structure that presents a permanent birefringence signal, we characterized the temperature dependence of the birefringence pattern. We performed differential scanning calorimetry (DSC) tests. The sample collected from the V-shaped zone presents an endothermic peak at 65 °Cn calorimetric thermograms upon heating, whereas the sample collected from the bulk (or out of this zone) shows no thermal peak (Figure 3a). Melting of crystallites of PVA with high degrees of hydrolysis has been previously studied by calorimetry. It was demonstrated that the PVA crystallites in PVA hydrogels melt at about 60 °C[24, 27] Thus our result indicates that strain-induced crystallization occurs during the puncture test. We confirmed by birefringence the melting of the V-shaped anisotropic zone upon heating (Figure 3b). The gel sample containing a V-shaped zone formed by puncture at 25 °C was heated up to and maintained at 40, 65, and 90 °C. Up to 40 °C the anisotropic zone remains almost the same size, while with further increase in temperature, its size, and intensity decrease, and it ultimately disappears upon heating to 90 °C (Figure 3b).

In order to evaluate the temperature effect on the SIC, the puncture tests were performed at different temperatures. At 25, 40, and 65 °C, we find qualitatively the same behavior: at the fracture point d_c, a crack initiation point having a lower birefringence intensity suddenly appears above the needle tip. One can correlate the size of the crystalline zone with the distance between the needle tip and the crack initiation position, ΔL, determined from the line profile of the birefringence intensity (see Figure S5). In Figure 3c, ΔL is plotted as a function of temperature. The value of ΔL decreases with temperature. At 70 °C, the birefringence intensity quickly disappears, similar to that for the PVA88, indicating that SIC does not occur, and the value of ΔL is considered as 0 mm.

This is the first time that we observed the very-large strain-induced crystallization in such dilute swollen PVA hydrogels (C_{PVA} = 6.6 %). An increase in the PVA polymer concentration due to crystallization is demonstrated spectroscopically by staining PVA. When the fractured gel sheet is immersed in a solution of Congo red, which is known to form a complex with PVA by hydrogen bonding[28], the red color is more intense at the position of the needle tip, indicating that the PVA concentration is locally increased in this area (Figure S6). We also found that by the addition of urea (swelling the as-prepared hydrogel in a urea solution (5 mol/L) for one week and then performing the puncture test), the V-shaped birefringence pattern is invisible after puncture. This evidence strongly suggests that the strain-induced crystallization is formed by the strong hydrogen bonding associations between the stretched PVA chains.

Here we propose a mechanism of local reinforcement of PVA99 hydrogel by SIC in Figure 3d. During the puncture, PVA polymer chains are highly stretched and oriented during indentation, especially at the needle tip, where the stress is concentrated. The strong hydrogen bonding between neighboring stretched chains could fix the strain and form crystallites. Until a critical extreme large strain is attained, SIC occurs in the polymer-rich region around the needle tip, providing additional physical crosslinks to locally reinforce the network. At the border of the crystalline and amorphous zones, the stress can now concentrate, and a crack can initiate, detected as above needle-tip fracture

point. After retraction of the needle, this crystallization structure does not relax and remains in the sample, observed as the V-shaped birefringence pattern. This displaced crack initiation is analogous to the side-way crack propagation observed in natural rubber exhibiting strain-induced crystallization[12, 29]. In an opened crack of natural rubber, a secondary crack tends to propagate in the direction parallel (side-way) to the stretching direction rather than in the perpendicular direction, to avoid breaking the tough crystallites formed at the crack tip[12]. This mechanism does not hold at temperatures above the melting temperature of the PVA hydrogen bonding. In a same manner as non-crystalline polymers including PVA88, the puncture stress concentrates at the needle tip, and a crack initiates there, without additional reinforcement effect.

It should be noted that both chain orientation and crystallization contribute to birefringence, and it is difficult to quantitatively separate their respective contribution during loading. After needle retraction, we can assume that the chain orientation reversibly recovers and birefringence disappears, while crystallization irreversibly maintains birefringence. We are not able to argue eventual reversible crystallization in this system.[3]

It is known that aqueous solutions of PVA with a high DH can exhibit phase separation followed by microcrystallite formation upon cooling (freezing), and that the phase separation/crystallization temperature increases with PVA concentration.[30,31] For the PVA concentration studied in this work (6.6 wt%), the critical crystallization temperature is expected to be below 5 °C, indicating that the SIC observed in this work at about 25 °C is not due to the low-temperature induced phase separation/crystallization. We confirmed that the SIC behavior was observed for PVA hydrogels with variable PVA concentrations (Figure S7).

We systematically investigated how SIC affects fracture resistance of PVA hydrogels with various crosslinking densities (illustrated as modulus changes). By plotting ΔL, distance of crack position to needle tip, as a function of modulus, we found $\Delta L \sim 4$ mm for a gel with $G' = 250$ Pa (Figure 4a (i)), and $\Delta L \sim 1$ mm for a gel with $G' > 900$ Pa for PVA99, (Figure 4a (ii)), demonstrating that the softer gel may form a larger crystalline zone upon large puncture deformation due to its large chain deformability (lower crosslinking density). The puncture force F and normalized stress were plotted as a function of indenter displacement for PVA88 and PVA99 with various moduli in Figure S8. The value of the normalized stress at rupture (maximum), $\frac{\sigma_c}{G'}$, which can be considered as a measure of the fracture resistance of the sample, is plotted as a function of gel modulus for PVA88 and PVA99 hydrogels (Figure 4b). For PVA88 hydrogels, which do not exhibit SIC, one can see that the fracture resistance is practically independent of the modulus, consistent with the results reported by Crosby et. al. for organogels of triblock polymers.[32] They found that $\frac{\sigma_c}{G'}$ was independent of modulus at values of the order of 100. We confirmed a similar independence of the modulus for polyacrylamide hydrogels and PDMS elastomers (Figure S9). However, while the values of $\frac{\sigma_c}{G'}$ for the PVA99 hydrogel is comparable at low G' (for $G' = 80$ Pa, is about 4000) to that of the PVA88, it then decreases with increasing modulus and reaches about 1000 for $G' = 2000$ Pa. This result suggests that the SIC occurring locally near the needle tip cannot reinforce the whole material as it displaces the crack nucleation process away from the needle tip in the amorphous region of hydrogels, leading to localized fracture.

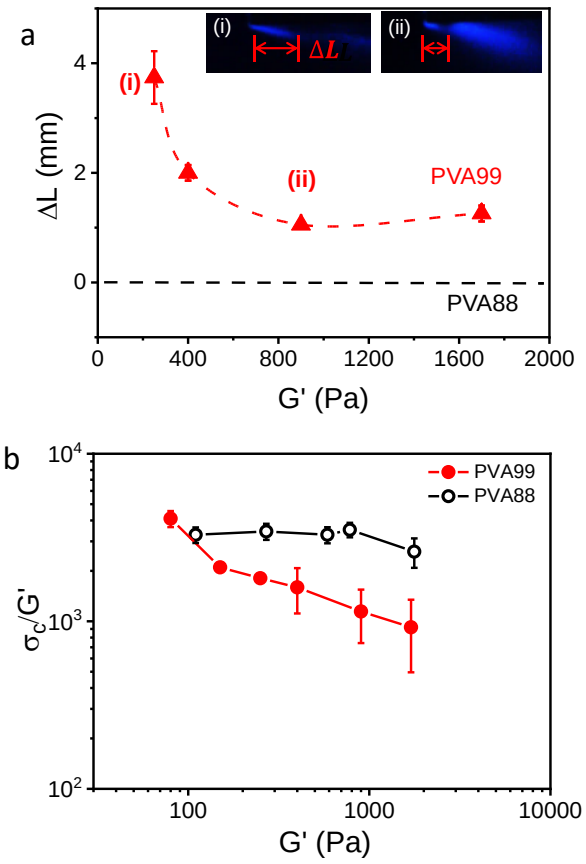

Figure 4. (a) Distance between needle tip and the crack initiation position, ΔL, as a function of G'. Birefringence at fracture point (i) G'=250 Pa and (ii) G'=1700 Pa. (b) Fracture resistance against G' for PVA88 and PVA99.

In conclusion, an unexpected needle-insertion-induced crystallization specifically in fully hydrolyzed PVA hydrogel can occur in the puncture geometry. This anisotropic crystalline structure can be introduced, even before fracture, by applying a large strain and is attributed to the strong hydrogen bonding associations between –OH groups on PVA chains. Owing to this SIC, the network around the needle is locally reinforced, displacing the crack initiation point from the needle tip to the edge. The geometry of indentation/puncture is very complex to further analyze the fracture mechanics, still, we believe that this work will motivate future studies of how specific microstructures can evolve in crystalline and associative polymers with extremely large deformation and contribute to a peculiar fracture behavior

in ultra-soft materials in general and especially in aqueous systems.

ASSOCIATED CONTENT

The Supporting Informatioin is available free of charge via the Internet at:
https://pubs.acs.org/10.1021/acsmacrolett.3c00343

AUTHOR INFORMATION

Corresponding Author

*Costantino.Creton@espci.fr, *Tetsuharu.Narita@espci.fr.

Author Contributions

TN designed the project. TN, JJ and YYW developed the experimental conditions and setups. TN and CC supervised the project. YYW performed the experiments. All the authors discussed the results and contributed to the final manuscript.

Funding Sources

Chinese Scholarship Council. European Union's Horizon 2020 Programme for Research and Innovation under the Marie Skłodowska-Curie Grant Agree-ment No. 765811(DodyNet). European Research Council (ERC) under the European Union's 2020 Research and Innovation Program (grant agreement no. 695351, CHEMECH). Agence Nationale de Recherche (GelWet, ANR-17-CE30-0016).

ACKNOWLEDGMENT

Yuanyuan Wei has benefitted from a scholarship from the Chinese Scholarship Council. Jianzhu Ju acknowledges support from European Union's Horizon 2020 Programme for Research and Innovation under the Marie Skłodowska-Curie Grant Agreement No. 765811(DodyNet). This project has received funding from the European Research Council (ERC) under the European Union's 2020 Research and Innovation Program (grant agreement no. 695351, CHEMECH). This project is partly supported by Agence Nationale de Recherche (GelWet, ANR-17-CE30-0016). The authors thank Donghao Zhao for preliminary preparation of some PVA samples.

REFERENCES

1. Lee, K. Y.; Mooney, D. J., Hydrogels for tissue engineering. *Chemical reviews* **2001,** *101* (7), 1869-1880.

2. Gong, J. P.; Katsuyama, Y.; Kurokawa, T.; Osada, Y., Double-network hydrogels with extremely high mechanical strength. *Advanced materials* **2003,** *15* (14), 1155-1158.

3. Liu, C.; Morimoto, N.; Jiang, L.; Kawahara, S.; Noritomi, T.; Yokoyama, H.; Mayumi, K.; Ito, K., Tough hydrogels with rapid self-reinforcement. *Science* **2021,** *372* (6546), 1078-1081.

4. Haraguchi, K.; Takehisa, T., Nanocomposite hydrogels: A unique organic – inorganic network structure with extraordinary mechanical, optical, and swelling/de - swelling properties. Adv. Mater. 2002, 14 (16), 1120-1124.

5. Creton, C., 50th anniversary perspective: Networks and gels: Soft but dynamic and tough. *Macromolecules* **2017,** *50* (21), 8297-8316.

6. Candau, N.; Laghmach, R.; Chazeau, L.; Chenal, J.-M.; Gauthier, C.; Biben, T.; Munch, E., Strain-induced crystallization of natural rubber and cross-link densities heterogeneities. *Macromolecules* **2014,** *47* (16), 5815-5824.

7. Trabelsi, S.; Albouy, P.-A.; Rault, J. J. M., Crystallization and melting processes in vulcanized stretched natural rubber. **2003,** *36* (20), 7624-7639.

8. Zhang, H.; Niemczura, J.; Dennis, G.; Ravi-Chandar, K.; Marder, M. J. P. r. l., Toughening effect of strain-induced crystallites in natural rubber. *Physical review letters* 2009, 102 (24), 245503.

9. Scetta, G.; Euchler, E.; Ju, J.; Selles, N.; Heuillet, P.; Ciccotti, M.; Creton, C., Self-Organization at the Crack Tip of Fatigue-Resistant Thermoplastic Polyurethane Elastomers. *Macromolecules* **2021,** *54* (18), 8726-8737.

10. Phillips, P.; Vatansever, N., Regime transitions in fractions of cis-polyisoprene. *Macromolecules* **1987,** *20* (9), 2138-2146.

11. Trabelsi, S.; Albouy, P.-A.; Rault, J., Crystallization and melting processes in vulcanized stretched natural rubber. *Macromolecules* **2003,** *36* (20), 7624-7639.

12. Lee, S.; Pharr, M., Sideways and stable crack propagation in a silicone elastomer. *Proceedings of the National Academy of Sciences* **2019,** *116* (19), 9251-9256.

13. Gent, A.; Kim, H., Tear strength of stretched rubber. *Rubber Chemistry and Technology* **1978,** *51* (1), 35-44.

14. Lin, S.; Liu, X.; Liu, J.; Yuk, H.; Loh, H.-C.; Parada, G. A.; Settens, C.; Song, J.; Masic, A.; McKinley, G. H., Anti-fatigue-fracture hydrogels. Science Advances 2019, 5 (1), eaau8528.

15. Lamberti, G., Flow induced crystallisation of polymers. *Chemical Society Reviews* **2014,** *43* (7), 2240-2252.

16. Bai, R.; Yang, J.; Suo, Z., Fatigue of hydrogels. *European Journal of Mechanics-A/Solids* **2019,** *74*, 337-370.

17. Wang, Z.; Zheng, X.; Ouchi, T.; Kouznetsova, T. B.; Beech, H. K.; Av-Ron, S.; Matsuda, T.; Bowser, B. H.; Wang, S.; Johnson, J. A., Toughening hydrogels through force-triggered chemical reactions that lengthen polymer strands. *Science* **2021,** *374* (6564), 193-196.

18. Barney, C. W.; Zheng, Y.; Wu, S.; Cai, S.; Crosby, A. J., Residual strain effects in needle-induced cavitation. *Soft Matter* **2019,** *15* (37), 7390-7397.

19. Fakhouri, S. M. Cavitation and Puncture for Mechanical Measurement of Soft Solids. University of Massachusetts Amherst, 2015.

20. Holloway, J. L.; Lowman, A. M.; Palmese, G. R., The role of crystallization and phase separation in the formation of physically cross-linked PVA hydrogels. *Soft Matter* **2013,** *9* (3), 826-833.

21. Auriemma, F.; De Rosa, C.; Triolo, R., Slow crystallization kinetics of poly (vinyl alcohol) in confined environment during cryotropic gelation of aqueous solutions. *Macromolecules* **2006,** *39* (26), 9429-9434.

22. Xie, X.; Wittmar, M.; Kissel, T., A Two-Dimensional NMR Study of Poly (vinyl (dialkylamino) alkylcarbamate-co-vinyl acetate-co-vinyl alcohol). *Macromolecules* **2004,** *37* (12), 4598-4606.

23. Briscoe, B.; Luckham, P.; Zhu, S., The effects of hydrogen bonding upon the viscosity of aqueous poly (vinyl alcohol) solutions. *Polymer* **2000,** *41* (10), 3851-3860.

24. Ilyin, S. O.; Malkin, A. Y.; Kulichikhin, V. G.; Denisova, Y. I.; Krentsel, L. B.; Shandryuk, G. A.; Litmanovich, A. D.; Litmanovich, E. A.; Bondarenko, G. N.; Kudryavtsev, Y. V., Effect of chain structure on the rheological properties of vinyl acetate–vinyl alcohol copolymers in solution and bulk. *Macromolecules* **2014,** *47* (14), 4790-4804.

25. Takamura, A.; Ishii, F.; Hidaka, H., Drug release from poly (vinyl alcohol) gel prepared by freeze-thaw procedure. *Journal of Controlled Release* **1992,** *20* (1), 21-27.

26. Toki, S.; Fujimaki, T.; Okuyama, M., Strain-induced crystallization of natural rubber as detected real-time by wide-angle X-ray diffraction technique. *Polymer* **2000,** *41* (14), 5423-5429.

27. Ricciardi, R.; Auriemma, F.; Gaillet, C.; De Rosa, C.; Lauprêtre, F. J. M., Investigation of the crystallinity of freeze/thaw poly (vinyl alcohol) hydrogels by different techniques. *Macromolecules* **2004,** *37* (25), 9510-9516.

28. Schütz, A. K.; Soragni, A.; Hornemann, S.; Aguzzi, A.; Ernst, M.; Böckmann, A.; Meier, B. H., The amyloid–Congo red interface at atomic resolution. *Angewandte Chemie International Edition* **2011,** *50* (26), 5956-5960.

29. Marano, C.; Calabrò, R.; Rink, M., Effect of molecular orientation on the fracture behavior of carbon black-filled natural rubber compounds. *Journal of Polymer Science Part B: Polymer Physics* **2010,** *48* (13), 1509-1515.

30. Liu, C.; Yu, X.; Li, Y.; Zhao, X.; Chen, Q.; Han, Y., Flow-induced crystalline precursors in entangled poly (vinyl alcohol) aqueous solutions. Polymer 2021, 229, 123960.

31. Joshi, N.; Suman, K.; Joshi, Y. M., Rheological behavior of aqueous poly (vinyl alcohol) solution during a freeze–thaw gelation process. Macromolecules 2020, 53 (9), 3452-3463.

32. Fakhouri, S.; Hutchens, S. B.; Crosby, A. J., Puncture mechanics of soft solids. *Soft Matter* **2015,** *11* (23), 4723-4730.

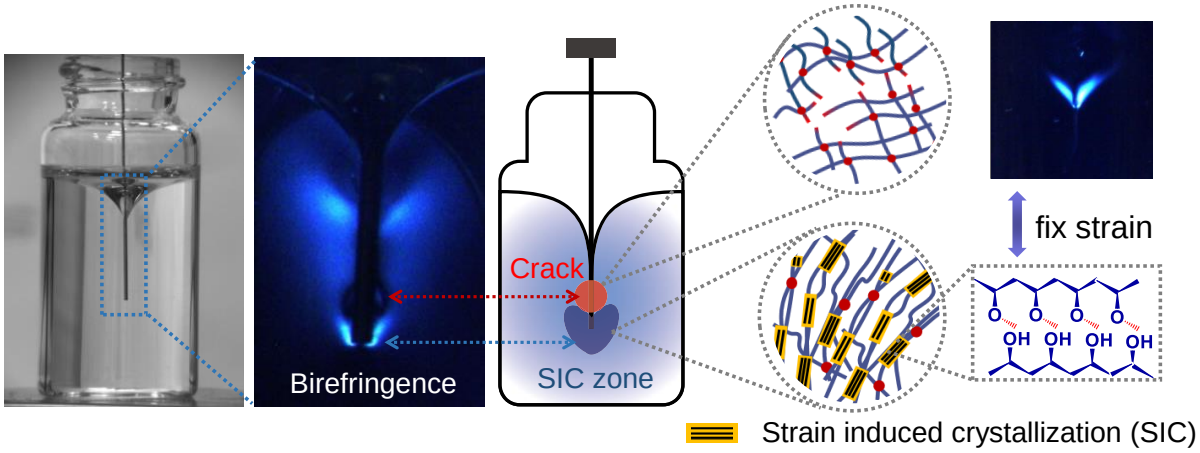
Birefringence
Crack
SIC zone
fix strain
O
OH
Strain induced crystallization (SIC)